Design of the low-IF filter for a ZigBee transceiver

A Project Report

submitted by

SHAIK ASIF BASHA

in partial fulfilment of the requirements
for the award of the degree of

MASTER OF TECHNOLOGY

DEPARTMENT OF ELECTRICAL ENGINEERING
INDIAN INSTITUTE OF TECHNOLOGY, MADRAS.

May 2008

THESIS CERTIFICATE

This is to certify that the thesis titled **Design of the low-IF filter for a ZigBee transceiver**, submitted by **Shaik Asif Basha**, to the Indian Institute of Technology, Madras, for the award of the degree of **Master of Technology**, is a bona fide record of the project work done by him under our supervision. The contents of this thesis, in full or in parts, have not been submitted to any other Institute or University for the award of any degree or diploma.

Dr. Nagendra Krishnapura
Project Adviser
Assistant Professor
Dept. of Electrical Engineering
IIT-Madras, 600 036

Place: Chennai
Date: 6th May 2008

ACKNOWLEDGEMENTS

I am grateful to Dr. Nagendra Krishnapura adviser, for his valuable guidance and encouragement throughout the duration of my project work.I was greatly benefited from the technical discussions I shared with them which helped me in understanding the finer aspects of circuit design. I am grateful to Dr. Shanthi Pavan for the technical discussions I shared on filter design.

Courses on Analog IC design and VLSI broadband circuits By Dr. Nagendra Krishnapura were the best classes I have ever taken. He introduced me to the area of analog IC design through his excellent classes and insightful assignments. His classes and the technical discussions I shared with him helped me a long way in the successful completion of this work. His consistency and dedication towards work is something which I hope to pick up. I thank my seniors J. Raja Prabhu and Sagar Kumar for helping me in the initial stages of my project. Thanks to Manoj, Karthik, Manohar, Bharadwaj, Abhishek Agrawal and Hari Prasath, for the technical discussions I had with them. Thanks to each and every one who helped me, in some way or the other, for successful completion of the project. Thanks to Abishek Goda for his help in understanding tools and analysis techniques. Thanks to Gargi Sharma for her help in preparing my thesis. Finally I dedicate this thesis to my parents for support and encouragement through all these years. This work would not have been possible without their love and understanding.

ABSTRACT

The project involves the design of a third order Butterworth complex filter to be used as part of the low-IF section of the receiver of the Zigbee Transceiver.

The purpose of the low-IF filter is not only to suppress high frequency components and extract required signal at IF after down convertion at the Mixer but also to reject the image signal situated at the same frequency but quadrature in nature. Design of the filter involves, design of two, two stage fully differential opamps used to implement complex biquad filter and first order complex filter, optimized for required linearity and noise specifications. The UGB of these opamps are 140MHz and 85MHz resp with power consumption $822\mu W$ and $861\mu W$. To avoid variations in the cutoff frequency of the filter across process and temperature variation, The filter is made tunable with a 4 bit control word. Power dissipation of the filter is $3.52mW$ with midband gain of $6dB$ and image rejection of $46dB$. Intput referred noise of the filter is $50nV/\sqrt{Hz}$ at 85° at RC maximum corner. Design, simulations and varifications were done in UMC 0.18μ technology with 1.8V supply voltage.

TABLE OF CONTENTS

LIST OF TABLES

LIST OF FIGURES

CHAPTER 1

Introduction

The work explained here is part of a project to design a low power IEEE 802.15.4(ZigBee) compliant transceiver to be used for wireless sensor applications operated by battery. The work details the design of complex filter used for low-IF transceiver. Its active-RC implementation and layout.

1.1 Organization of thesis

Chapter2 explains few basic concepts in complex signal processing, introduces to low-IF receiver architecture of the transceiver.

Chapter3 discusses complex filter design.

Chapter4 explains the design of low pass filter, including the op-amps used in the filter and process varieations and filter tuning.

Chapter5 discusses simulation results, layout, conclusion and future developments.

Chapter6 concludes the project with future work.

CHAPTER 2

Complex Signal Processing

Wireless systems often make use of the quadrature relationship between pair of signals to effectively cancel out of band and interfering in band signal components. The understanding of these systems is simplified by considering both the signal and system transfer functions as complex. This approach is very useful in highly integrated multistandard receivers where the use of the narrow band fixed coefficient filters at RF and high IF frequencies must be minimized.

2.1 Complex Signals

A complex signal(1) consists of a pair of real signals at an instance in time. The mathematical representation of this signal is given as

$$x(t) = x_r(t) + jx_i(t) \tag{2.1}$$

where $j = \sqrt{-1}$. In an actual physical system the signals are both real (but are called real and imaginary parts) and are found in two distinct signal paths. The multiplier j is used to help define operations between different complex signals. It allows for image-rejection architectures to be described more compactly and simply.

2.2 Mathematical operations on complex signals

2.2.1 Complex addition

The mathematical representation of complex addition is given as

$$y(t) = x_1(t) + x_2(t) = (x_{1r}(t) + x_{2r}(t)) + j(x_{1i}(t) + x_{2i}(t)) \tag{2.2}$$

The signal flow graph of the complex signal adder is in Fig. 2.1

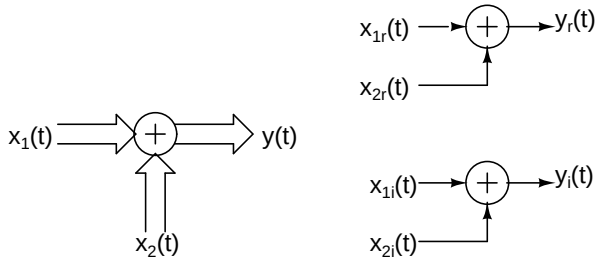

Figure 2.1: Complex addition

2.2.2 Complex multiplication

The mathematical representation of complex multiplication is given as

$$y(t) = x(t)X(a + jb) = (ax_r(t) - br_i(t)) + j(ax_i(t) + bx_r(t)) \tag{2.3}$$

The signal flow graph of the complex signal multiplier is in Fig. 2.2

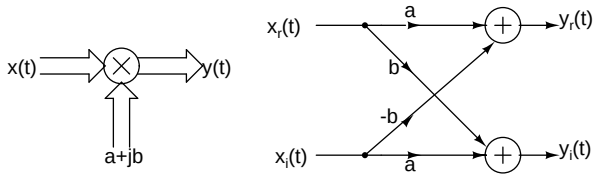

Figure 2.2: Complex multiplication

A special case of complex multiplication in complex signal processing is the

image rejection mixer which is very widely used in modern receivers. The mathematical representation of this image rejection mixer is given as

$$y(t) = x_{RF}(t)e^{-j\omega_{LO}t} = x_{RF}(t)cos(\omega_{LO}t) - jx_{RF}(t)sin(\omega_{LO}t) \tag{2.4}$$

The frequency domain representation of the above time domain representation is given as

$$Y(\omega) = X_{RF}(\omega - \omega_{LO}) \tag{2.5}$$

The signal flow graph of the image rejection mixer is as in Fig. 2.3.

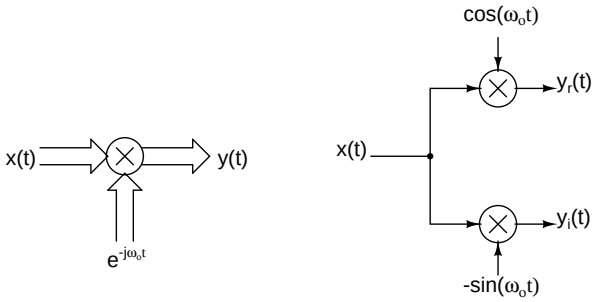

Figure 2.3: Image rejection mixer

The amplitude spectrum of the $x_{RF}(t)$ and $y(t)$ are shown in Fig. 2.4.

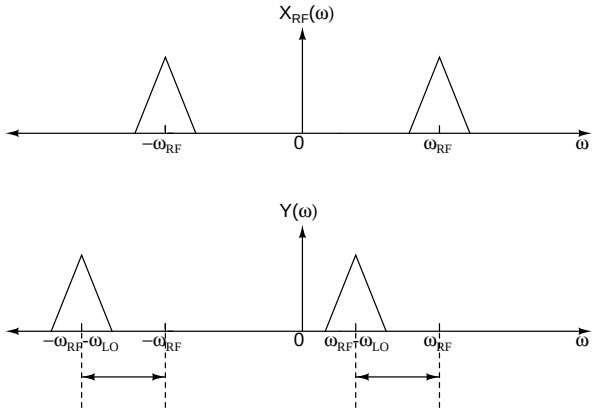

Figure 2.4: Frequency domain representation of image rejection mixing

One more important special case of the complex multiplication is multiplication by $j = \sqrt{-1}$ which is very widely used in complex filter design. The time domain

mathematical representation is given as

$$y(t) = jx(t) = j(x_r(t) + jx_i(t)) = -x_i(t) + jx_r(t) \tag{2.6}$$

Multiplication by j introduces a phase shift of 90° to the signal. The signal flow graph of this operation is shown in Fig. 2.5

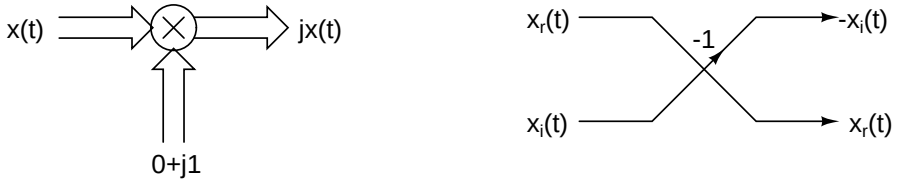

Figure 2.5: Signal multiplication by j

2.2.3 Complex Conjugate

The complex conjugate operation on complex signal is mathematically given as

$$x(t) = Me^{j(\omega_o t + \phi)} \tag{2.7}$$

$$x^*(t) = Me^{-j(\omega_o t + \phi)} \tag{2.8}$$

The signal flow graph of the complex conjugate operation is shown in Fig. 2.6. The complex conjugate operation on a complex signal results in frequency scale

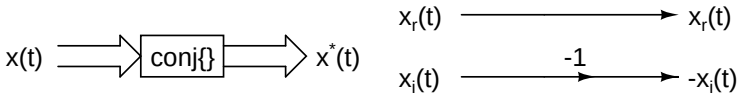

Figure 2.6: Complex conjugation

reversal in frequency domain. It is as shown in Fig. 2.7.

$$X^*(\omega) = X(-\omega) \tag{2.9}$$

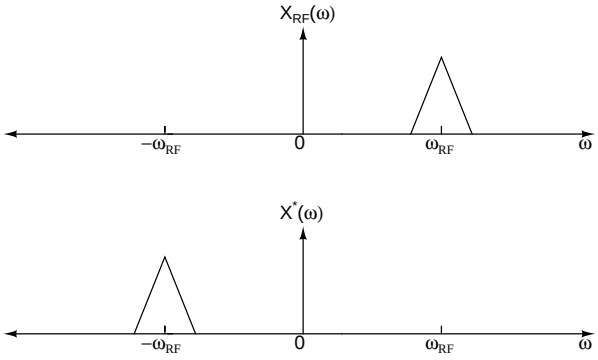

Figure 2.7: Frequency domain representation of complex conjugate operation

2.3 Complex integrator

The complex integrator(2) is a basic building block of a complex filter. Any low-pass prototype can be modified as a complex bandpass filter by frequency shifting a real integrator to a desired frequency which will be the center frequency of the resultant bandpass complex filter. The transfer function of the complex integrator is given as

$$I_c(s) = \frac{\omega_o}{s - j\omega_c} \tag{2.10}$$

Its block diagram is shown in Fig. 2.8. The complex signal flow graph of this

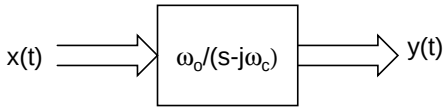

Figure 2.8: Complex integrator block

integrator is given as in Fig. 2.9. The above complex signal flow graph can be

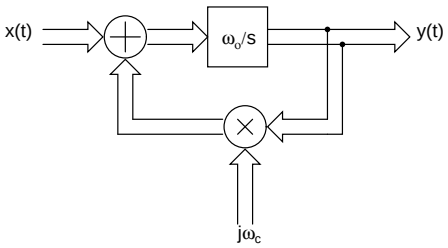

Figure 2.9: Complex integrator

transformed into a real signal flow graph by implementing multiplication by j in it. Then the complex integrator can be shown as in Fig. 2.10. The frequency

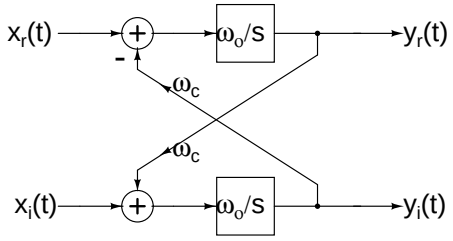

Figure 2.10: Real SFG of complex integrator

response of real integrator and complex filter centered at $\omega_c = 2\pi \times 2.5MHz$ is in Fig. 2.11.

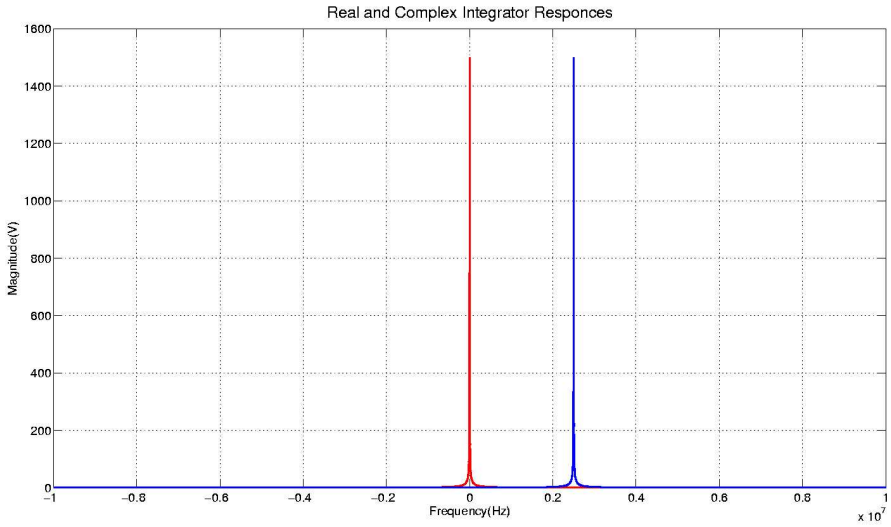

Figure 2.11: Real and complex integrator spectrum

2.4 Mismatch in complex signal processing

The presence of mismatch(3) between real and imaginary paths results in improper image rejection. This phenomenon can be explained by using mismatch in two amplifiers in real and imaginary paths. The mismatch between two amplifiers can be modeled as two parallel complex paths, one with no mismatch and another with only mismatch term as shown in Fig. 2.12. The presence of complex conjugate

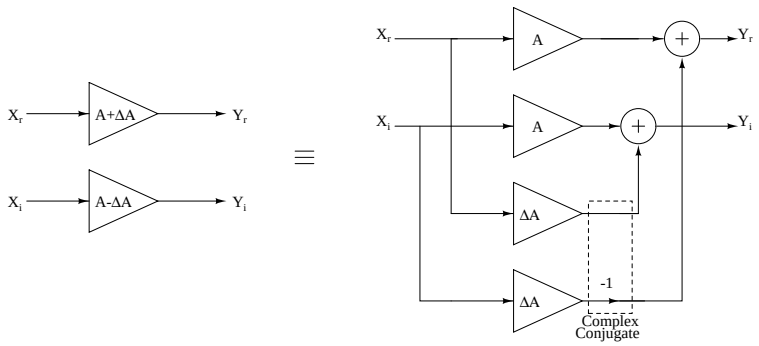

Figure 2.12: Mismatch in amplifiers

operation in mismatch path results in frequency mirroring which in turn results in uncanceled image with a gain of ΔA at the output. Hence the image rejection is given as $\frac{\Delta A}{A}$.

2.5 Low-IF receiver architecture

Low-IF receivers are an alternative(2) to Zero-IF receiver architecture for wireless transceivers with a high degree of integration. The low-IF architecture overcomes inherent drawbacks in the zero-IF receiver architecture.

In zero-IF architecture the RF signal will be directly down converted to baseband and further signal processing takes place at baseband which is very much prone to nonlinearity. The reason for the nonlinearity is the presence of dc offset generated at the output of down conversion mixer because of the mixing of local oscillator output given to mixer and leakage between local oscillator output and RF input of the mixer. In low-IF receiver the RF signal will be down converted to an intermediate frequency. The intermediate frequency in general will be comparable to the bandwidth of the signal. The main advantage of the low-IF compared to direct conversion or zero-IF receiver is that the dc offset from mixer gets attenuated and singal is less affected by $\frac{1}{f}$ noise. The basic receiver block diagram of the low-IF receiver is shown in Fig. 2.13.

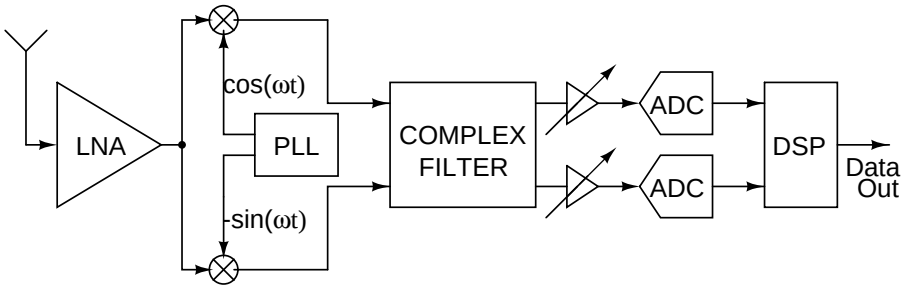

Figure 2.13: Low-IF receiver architecture

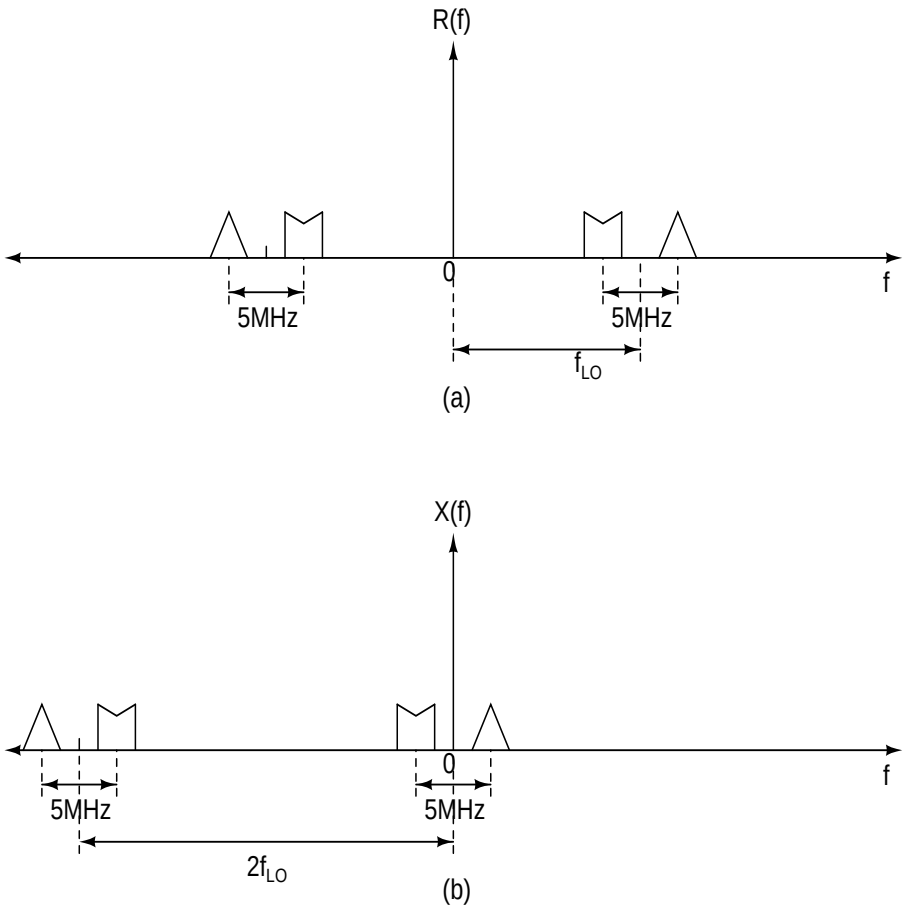

Figure 2.14: Signal spectrum input and output of image rejection mixer

It is easy to understand the functionality of the low-IF architecture by looking at the signal spectrum at different stages of the receiver. The spectrum of the received signal before and after the image rejection mixer is shown in Fig. 2.14. After down conversion the the required signal and its adjscent channel are situated at 2.5MHz and -2.5MHz as shown in Fig. 2.15(a). To filter out image signal which is situated at -2.5MHz while preserving the required signal at 2.5MHz, a complex filter with asymmetric frequency response which processes complex signals is necessary. The frequency response of such complex filter is in Fig. 2.15(b). The spectrum of the output complex signal of the complex filter is shown in Fig. 2.15(c).

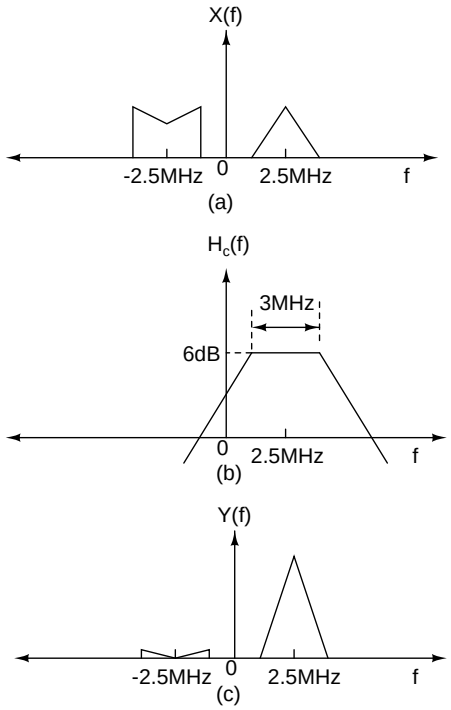

Figure 2.15: Signal spectrum at input and output of complex filter

Next chapter discusses the design of the complex filter for the ZigBee transceiver.

CHAPTER 3

Complex Filter

The low-IF complex filter is being used not only to attenuate the signals of out of the band of interest but also to filter the required signal at intermediate frequency ω_c from its image signal at $-\omega_c$ after down conversion. The bandwidth of the complex filter for low-IF ZigBee chip is 3MHz centered at 2.5MHz. The lowpass prototype of the complex filter is the 3^{rd} order Butterworth filter of cutoff frequency at 1.5MHz. The dynamic range of the filter is 52dB. Hence opamp RC filter implementation is preferred over g_mC implementation.

3.1 Choice of topology

In general a complex filter can be implemented by frequency transforming a prototype lowpass filter implemented in standard state space with integrators as basic building blocks to the desired intermediate frequency. This can be done by replacing the normal integrator with a complex integrator centered at intermediate frequency(ω_c). Hence to implement a third order Butterworth filter we require six opamps which consumes lot of power. For a ZigBee receiver where the power consumption is a very important specification a topology which has lesser opamps is preferable. Hence the 3^{rd} order filter is implemented using a first order complex filter followed by a complex biquad which requires four opamps. The first stage is a first order complex filter with gain 2. The reason for providing this gain for the first stage of the filter is to reduce the input referred noise of the biquad which is noisy compared to the first order complex filter.

3.2 Filter design

The transfer function of the complex Butterworth filter is given as

$$H_c(s') = \frac{A}{(s'/\omega_o)^3 + 2(s'/\omega_o)^2 + 2(s'/\omega_o) + 1}$$

$$\begin{aligned} \text{Where} \quad s' &= s - j\omega_c \\ \omega_o &= 2\pi \times 1.5 \times 10^6 rad/sec \\ \omega_c &= 2\pi \times 2.5 \times 10^6 rad/sec \\ A &= 2 \end{aligned}$$

3.2.1 First order complex filter design

The filter comprises a first order complex filter followed by a complex biquad. The first order complex filter was designed by transforming a lowpass prototype filter with gain 2 and cutoff frequency 1.5MHz to the intermediate frequency 2.5MHz. The first order transfer function of the complex filter is

$$H_{c1}(s) = \frac{A}{1 + \frac{s - j\omega_c}{\omega_o}} \tag{3.1}$$

$$\begin{aligned} \text{Where} \quad A &= 2 \\ \omega_o &= 2\pi \times 1.5 \times 10^6 \\ \omega_c &= 2\pi \times 2.5 \times 10^6 \end{aligned}$$

The first order complex filter is shown in Fig. 3.1.

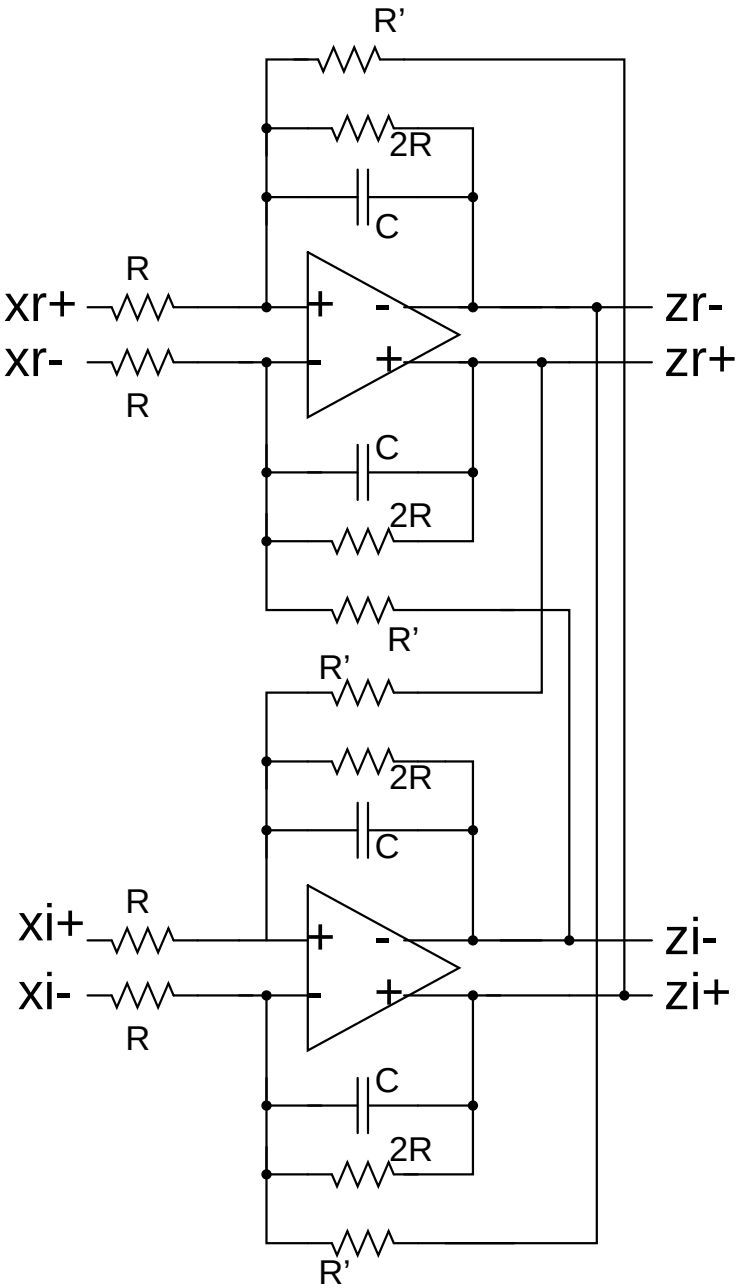

Figure 3.1: First order complex filter

The transfer function of the complex filter in terms of components is

$$H_c(s) = \frac{2}{1 + 2RC(s - j\omega_c)}$$

$$\begin{aligned} \text{Where} \quad R &= 5.2K\Omega \\ \omega_o &= 2\pi \times 1.5 \times 10^6 \\ \omega_c &= 2\pi \times 2.5 \times 10^6 \\ 2RC &= \frac{1}{\omega_o} \\ R' &= \frac{1}{\omega_c C} \end{aligned}$$

The frequency response of the first order complex filter is shown in Fig. 3.2.

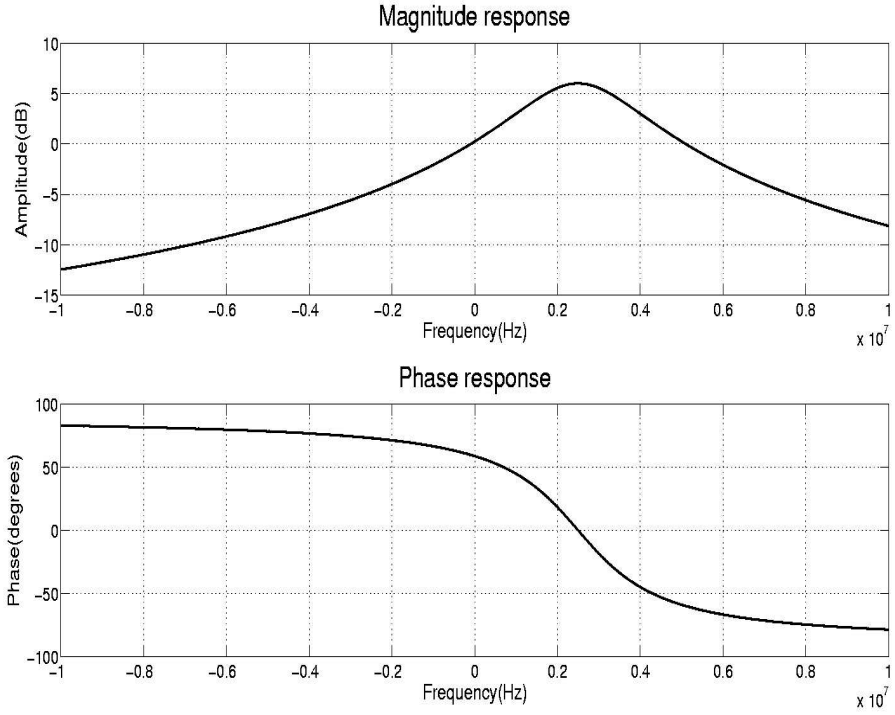

Figure 3.2: Frequency response of first order complex filter

From above equations the component values are calculated and they are as in

Table. 3.1. The value of resistance R is $5.2K\Omega$ because it is the load resistance of the current output mixer.

Table 3.1: Resistor and capacitor values for the first order complex filter

Components	*values*
R	$5.2K\Omega$
C	$10.2pF$
R'	$6.24K\Omega$

3.2.2 Complex biquad design

The complex biquad schematic is shown as in Fig. 3.3.

The transfer function of this complex biquad is given as

$$H_c(\omega) = \frac{A}{(1 - \frac{j(\omega-\omega_c)}{a+jb})(1 - \frac{j(\omega-\omega_c)}{a-jb})} \tag{3.2}$$

which is the frequency transformation to intermediate frequency ω_c of the real biquad of transfer function given below

$$H_c(\omega) = \frac{A}{(1 - \frac{j\omega}{a+jb})(1 - \frac{j\omega}{a-jb})} \tag{3.3}$$

Here ω_c is normalized with respect to lowpass prototype cutoff frequency ω_o. For a 3^{rd} order Butterworth filter $a+jb$ and $a-jb$ are the roots the biquad polynomial $s^2 + s + 1$.

The design formulas(2) for the complex biquad are as follows.

$$X = \frac{2a + \sqrt{(2a)^2 + 4(\omega_c^2 - (a^2 + b^2))}}{2} \tag{3.4}$$

$$Y = X - 2a \tag{3.5}$$

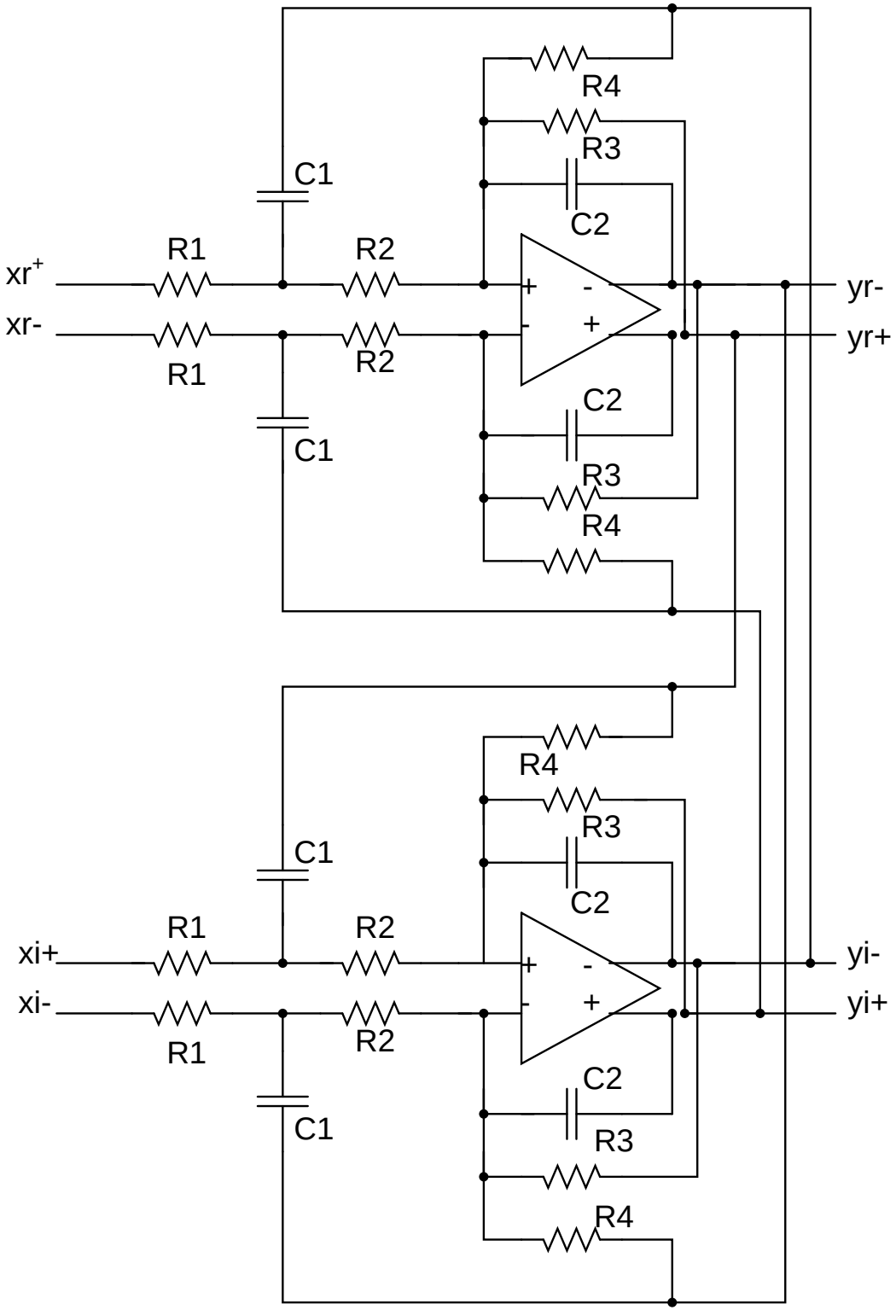

Figure 3.3: Complex biquad filter

$$Z = \frac{2a\omega_c}{X} \tag{3.6}$$

$$C_1 = \frac{2\omega_c - Z(a^2 + b^2)}{a^2 + b^2} \tag{3.7}$$

$$C_2 = \frac{1}{(a^2 + b^2)C_1 R_2} \tag{3.8}$$

$$R_1 = \frac{1}{A} \tag{3.9}$$

$$R_2 = \frac{1}{XC_1 - \frac{1}{R_1}} \tag{3.10}$$

$$R_3 = \frac{1}{YC_2} \tag{3.11}$$

$$R_4 = \frac{1}{ZC_2} \tag{3.12}$$

By using above formulas the complex biquad can be designed for $A = 1$ and $\omega_c = \frac{2.5}{1.5}$. After obtaining the normalized values of the components of the complex biquad, the resistances are demoralized by multiplying them by impedance factor $IF = 32K|Omega$ and the capacitances are scaled by dividing them by $IF \times \omega_o$ where $\omega_o = 2\pi \times 1.5MHz$

Table 3.2: Resister and capacitor values for complex biquad

Components	*values*
R_1	$32K\Omega$
R_2	$8.54K\Omega$
R_3	$22.8K\Omega$
R_4	$24.3K\Omega$
C_1	$8.18pF$
C_2	$5.03pF$

The frequency response of the complex biquad is shown in Fig. 3.4.

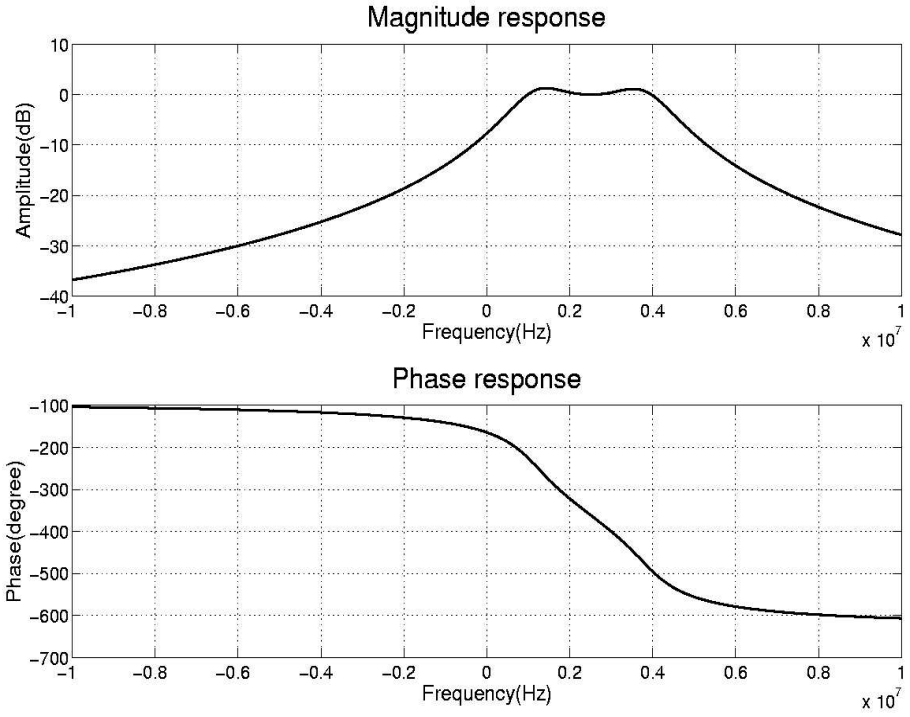

Figure 3.4: Complex biquad frequency response

3.3 Complete filter

The complete filter is shown in Fig. 3.5. Here X_r and x_i corresponds to the real part of input complex signal and y_r and $Y - i$ are the real and imaginary parts of the output complex signal. The expressions for the frequency responce calculation after Ac analysis is

$$Magnitude = 20 \times \log_{10}\left(\frac{(y_r + jr_i)}{(x_r + jx_i)}\right) \tag{3.13}$$

$$Phase = arg\left(\frac{(y_r + jr_i)}{(x_r + jx_i)}\right) \tag{3.14}$$

The response of the filter in shown in Fig. 3.6

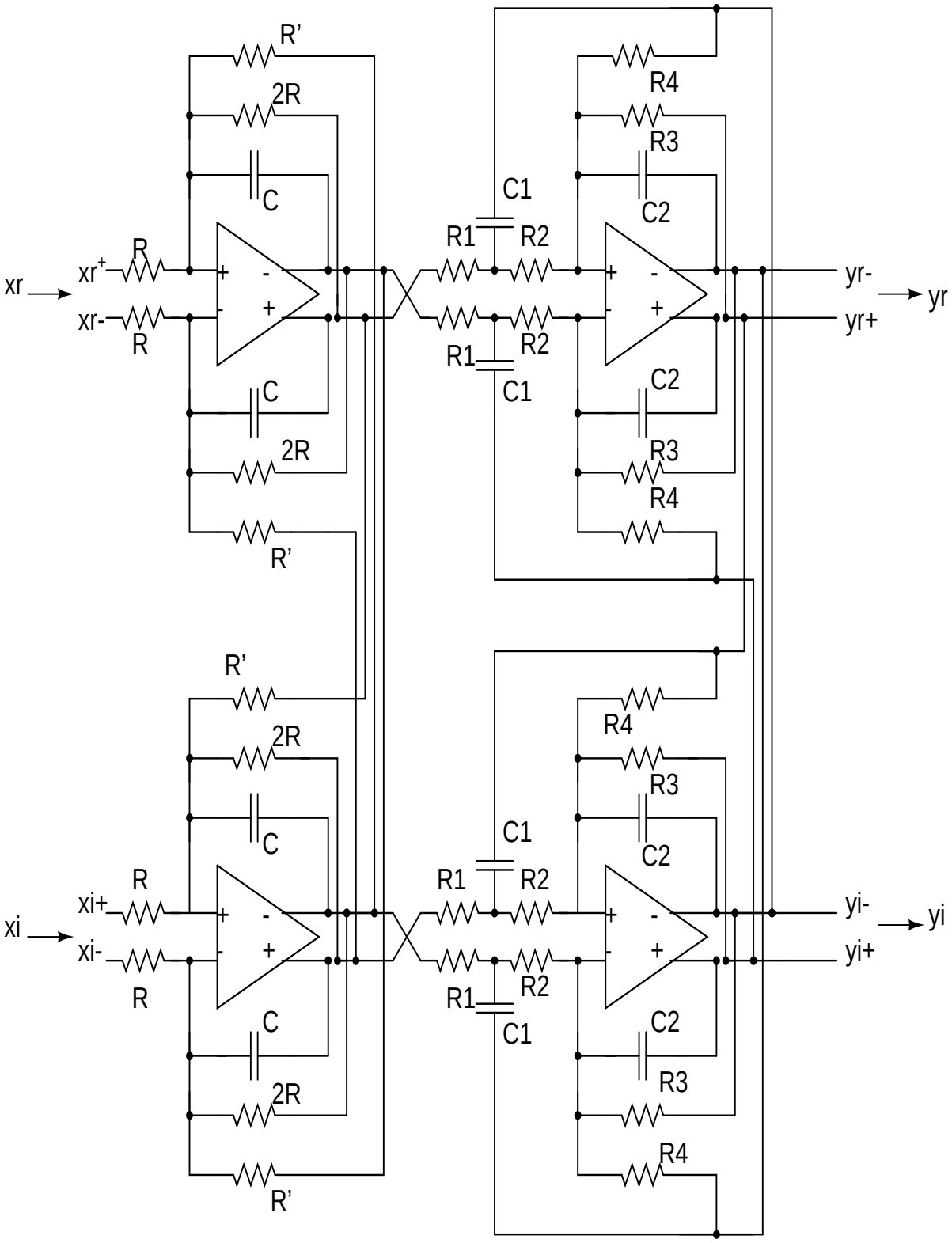

Figure 3.5: 3^{rd} order complex Butterworth filter

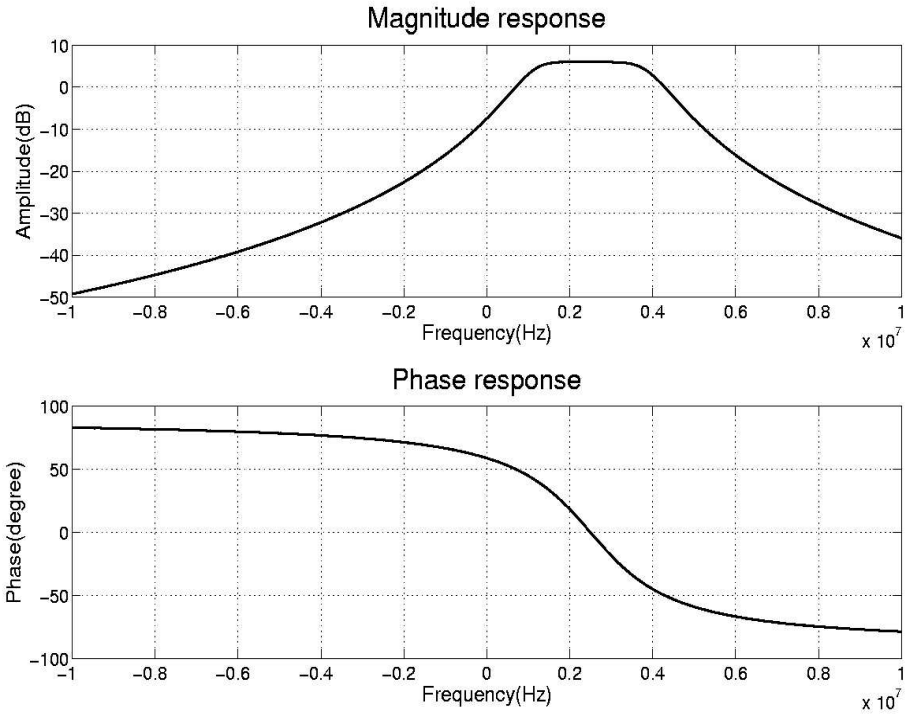

Figure 3.6: Ideal magnitude and phase response

3.4 Noise consideration

Unlike zero-IF section in the low-IF architecture both I and Q channels interact with each other for image cancellation, hence each resistance from I channel will not only contribute to noise at output of I channel but also to the noise at Q channel output and vice versa. The output noise because of the complex biquad filter is many folds compared to the output noise because of the the first order filter. The major contributor of noise is the resistance R_2. The noise transfer function of the filter from the resistance R_2 in Q channel to any one of the outputs of I channel is shown in Fig. 3.7. The peak gain of the the noise because of this resistance is $20dB$ at the center frequency of the low-IF filter(2.5MHz). This topology if used with unity gain will undermine the required SNR specification.

To overcome this limitation first order filter which precedes this complex biquad was designed for gain equal to two. In principle the gain of the complex filter can be increased till we don't provide additional gain to the dc offset.

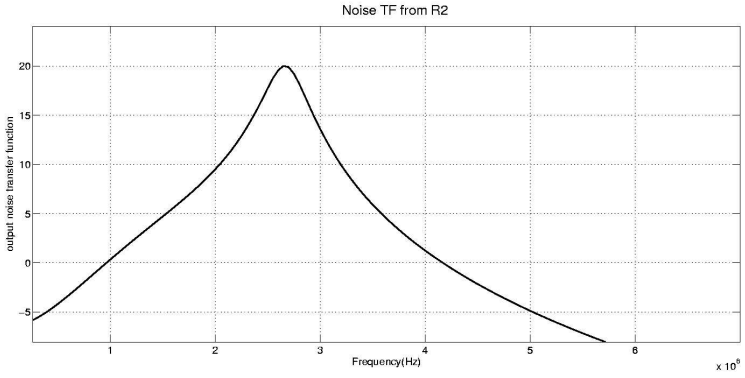

Figure 3.7: Noise transfer function from R_2 to output

CHAPTER 4

Opamp Design

This chapter discusses the design of two opamps designed for implementing complex filter and tuning capacitor bank for process variations.(4).

4.1 Opamp design for complex biquad

The noise contribution because of the biquad is higher than the first order complex filter. The opamp designed to implement the complex biquad was optimized for minimum noise. Since the filter being implemented is low-IF, the amount of output noise contributed by thermal noise because of resistances and transistors is more than the $\frac{1}{f}$ noise because of the transistors. To reduce the effect of thermal noise the first stage of both the opamps were implemented using N-channel MOSFETs.

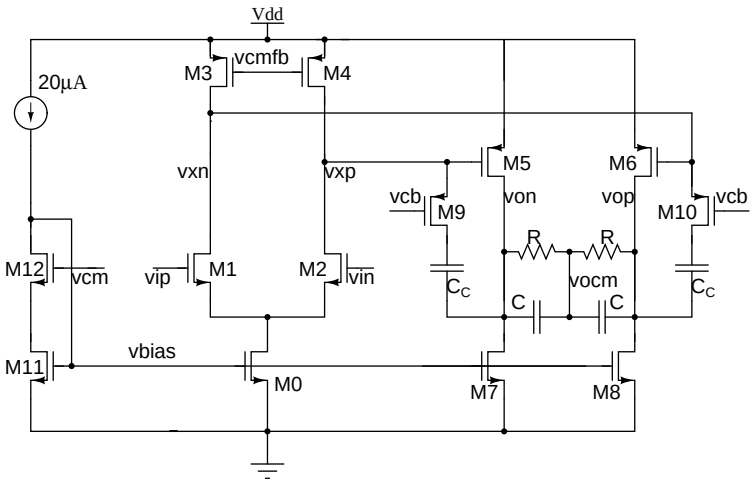

Figure 4.1: Opamp used for complex biquad

The schematic of the two stage opamp used for biquad implementation is shown in Fig. 4.1. The dimensions of the transistors of opamp are as in Tab. 4.1.

Table 4.1: Transistor sizing of opamp for complex biquad

Transistor	Parameters	
	Finger dimensions	No. of fingers
M0	$2\mu/0.4\mu$	8
M1,M2	$15\mu/0.56\mu$	8
M3,M4	$0.4\mu/0.7\mu$	8
M5,M6,M9,M10	$4.4\mu/0.4\mu$	10
M7,M8	$2\mu/0.4\mu$	14
M11	$2\mu/0.4\mu$	2
M12	$15\mu/0.56\mu$	2
M13	$2\mu/0.4\mu$	2
M14,M15	$15\mu/0.56\mu$	2
M16,M17	$0.4\mu/0.7\mu$	2
M18	$2\mu/0.4\mu$	2
M19,M20	$3.14\mu/0.4s\mu$	2

The commonmode feedback of the circuit is shown in Fig. 4.2. The compensation of the two stage opamp was done by compensation capacitor C_c and MOSFET resistors M9(and M10). The biasing circuit for M9(and M10) is shown in Fig. 4.3.

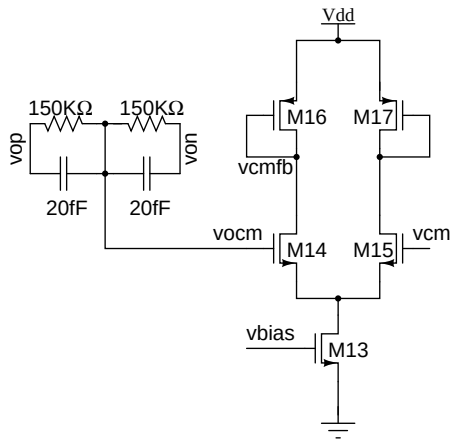

Figure 4.2: Common-mode feedback circuit

The frequency response of the opamp is shown in Fig. 4.4. The commonmode feedback impulse response is shown in Fig. 4.5.

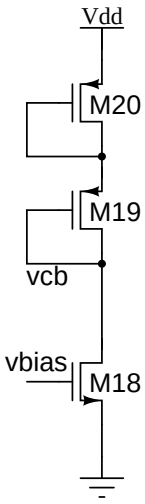

Figure 4.3: Compensation MOSFETs bias generation circuit

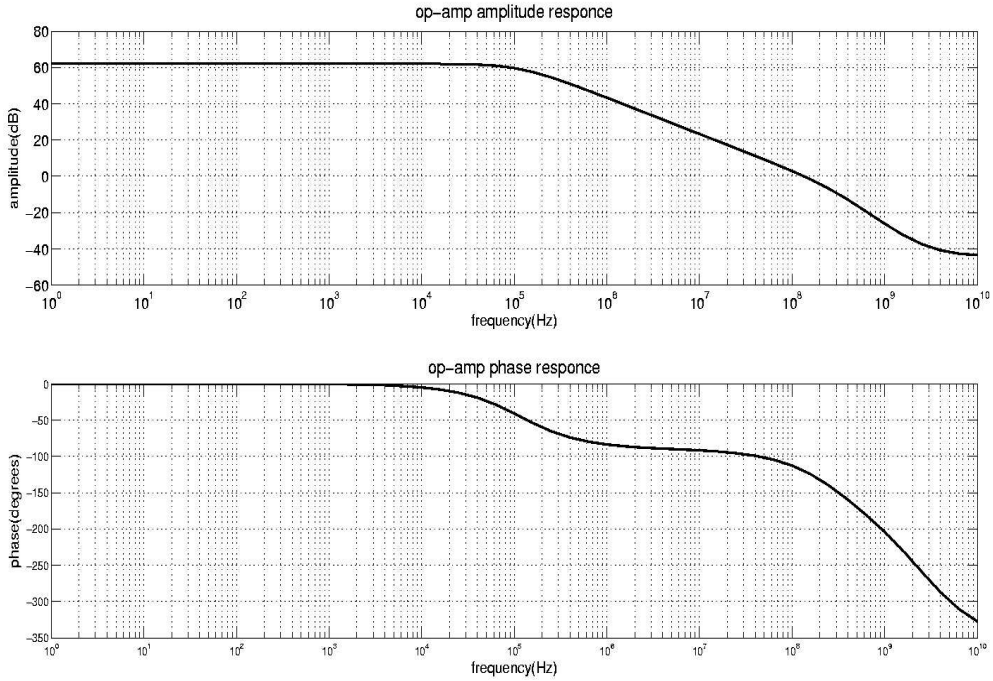

Figure 4.4: Opamp frequency response

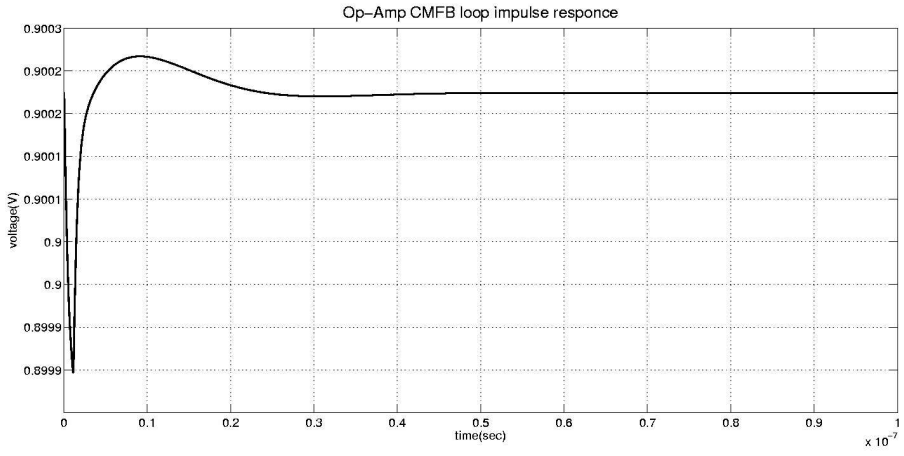

Figure 4.5: Opamp CMFB stability

Table 4.2: Specifications of opamp

DC gain	$62dB$
UGB	$140MHz$
Phase margin	$60°$
Power consumption	$822\mu W$
THD (unity feedback with feedback resistor of $10K\Omega$ at $700mV$ peak to peak output)	$-82dB$

Some of the important specifications of the opamp are tabulated in Tab. 4.2.

4.2 Opamp design for first order complex filter

The first order complex filter is less noisy compared to the complex biquad. Hence to reduce the filter's input referred noise because of the complex biquad the first order filter which precedes the complex provides gain of 2 to the IF signal. This reduces the noise power because of complex biquad referred to input of the filter by four times. Because of this gain of 2 the complex first order filter has to support maximum output swing of 700mV peak to peak with resistive loading of 3.9K(2.73K at minimum resistance corner) and capacitance of 10.2pF with sufficient linearity.

The schematic of this opamp is shown in Fig. 4.6

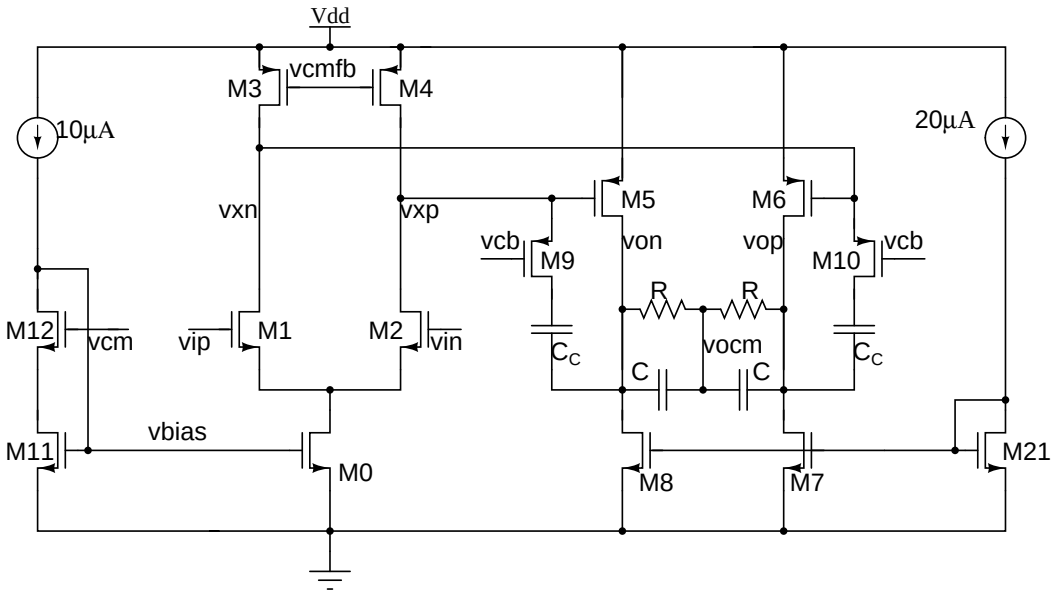

Figure 4.6: Opamp for first order complex filter

CMFB circuit for this opamp is shown in Fig. 4.2. The bias generation circuit for compensation MOSFET resistance is shown in Fig. 4.3. The transistor sizes of this opamp are given in Tab. 4.3.

The frequency response of this opamp is shown in Fig. 4.7. The impulse response of the common mode feedback circuit is shown in Fig. 4.8.

The specifications of the opamp used for 1^{st} order complex filter is in Tab. 4.4.

4.3 Process variations and filter tuning

For the realization of the filter polysilicon resistors are used which vary across process and temperature. The variation in resistance is about ±30% around typical value. The variation in capacitance is around ±15%. The uncompensated filter's frequency response deviates from the designed. For the complex filter the typ, max and min values of capacitances and resistances result in frequency response shown in Fig. 4.9.

Table 4.3: Transistor sizes of opamp for biquad

Transistor	Parameters	
	Finger dimensions	No. of fingers
M0	$2\mu/0.6\mu$	4
M1,M2	$5\mu/1\mu$	8
M3,M4	$1\mu/0.24\mu$	12
M5,M6,M9,M10	$2\mu/0.26\mu$	24
M7,M8	$2\mu/0.6\mu$	14
M11	$2\mu/0.6\mu$	4
M12	$5\mu/1\mu$	16
M13	$2\mu/0.6\mu$	2
M14,M15	$5\mu/1\mu$	4
M16,M17	$0.24\mu/1\mu$	6
M18	$1\mu/0.6\mu$	2
M19,M20	$.24\mu/0.26s\mu$	24
M21	$1\mu/0.6\mu$	2

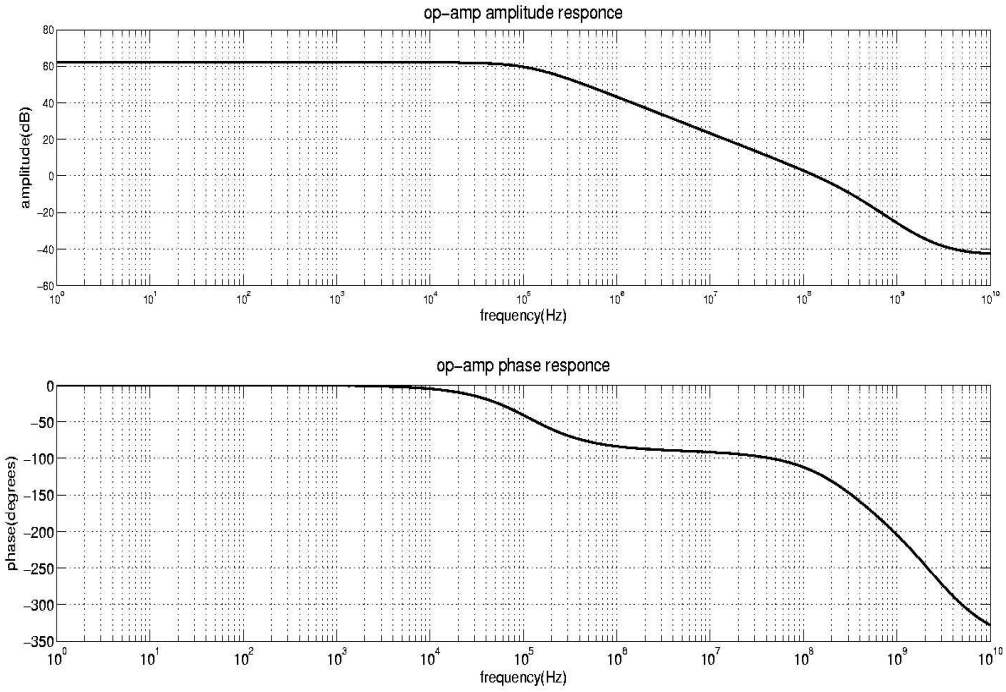

Figure 4.7: Opamp frequency response

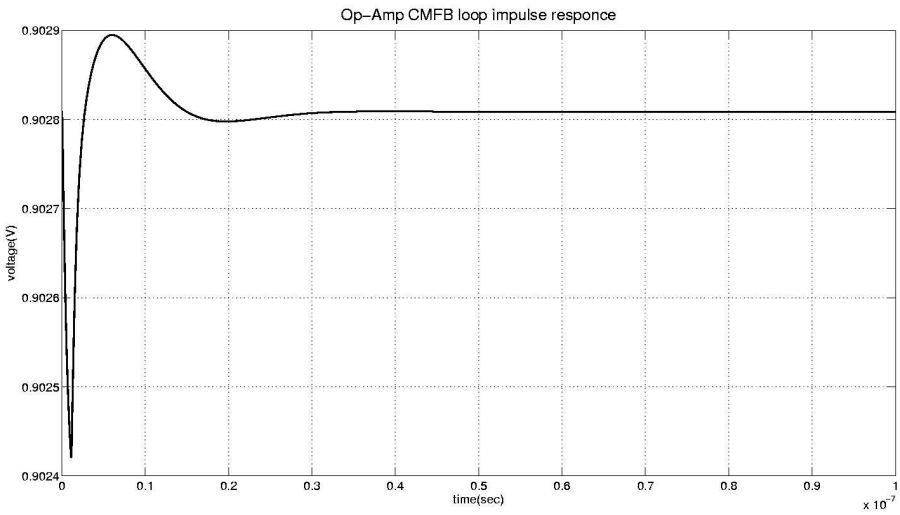

Figure 4.8: Stability of CMFB loop

Table 4.4: Specifications of opamp used for first order complex filter

DC gain	$68.5dB$
UGB	$85MHz$
Phase margin	$57.2°$
Power consumption	$861.3\mu W$
THD (unity feedback with feedback resistance of $5K\Omega$ at $700mV$ peak to peak output)	$-82dB$

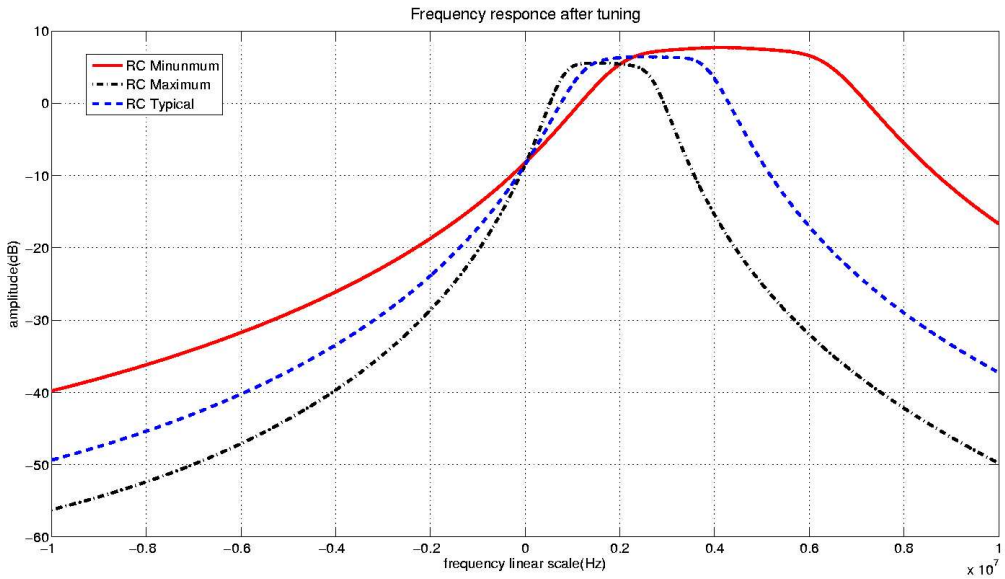

Figure 4.9: Frequency response deviation over process variations

Table 4.5: Capacitor bank values

Capacitor	C_{min}	ΔC
C	$6.76pF$	$641fF$
C_1	$5.72pF$	$536fF$
C_2	$3.5pF$	$332fF$

To compensate these process variations programmable capacitors are used. Depending on the on chip resistance and capacitance, capacitor bank is programmed to restore the required frequency response of the filter. A typical capacitance bank is shown as in Fig. 4.10.

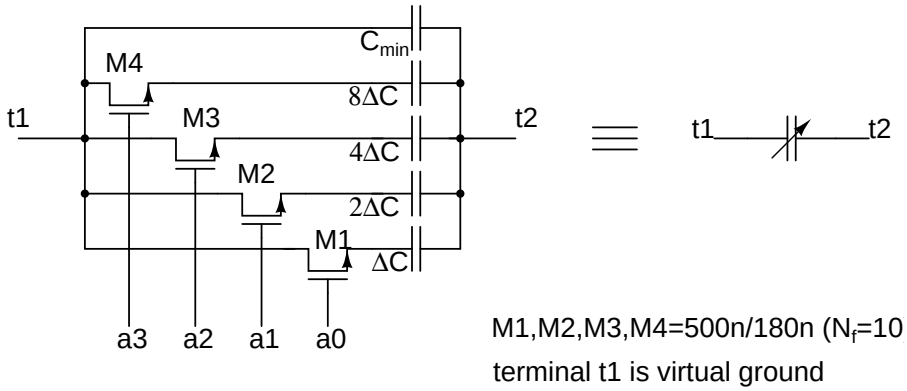

Figure 4.10: Capacitor bank for tuning filter

The value of C_{min} has been chosen such that it perfectly tunes the filter to the required time constant at the highest time constant over process variations. The value of capacitance ΔC has been chosen such that parallel combination of all the capacitors in capacitance bank $C = C_{min} + 15\Delta C$ tunes the filter to the required transfer function at the lowest time constant over process variation. The capacitor bank values of the tunable filter are in Tab. 4.5. The variables in above Tab. 4.5 are referred to the schematic diagram in Fix. 3.5.

The frequency response of the complex filter after tuning over extreme time constants is shown in Fig. 4.11. The maximum deviation in cutoff frequencies of the filter is 3.4%.

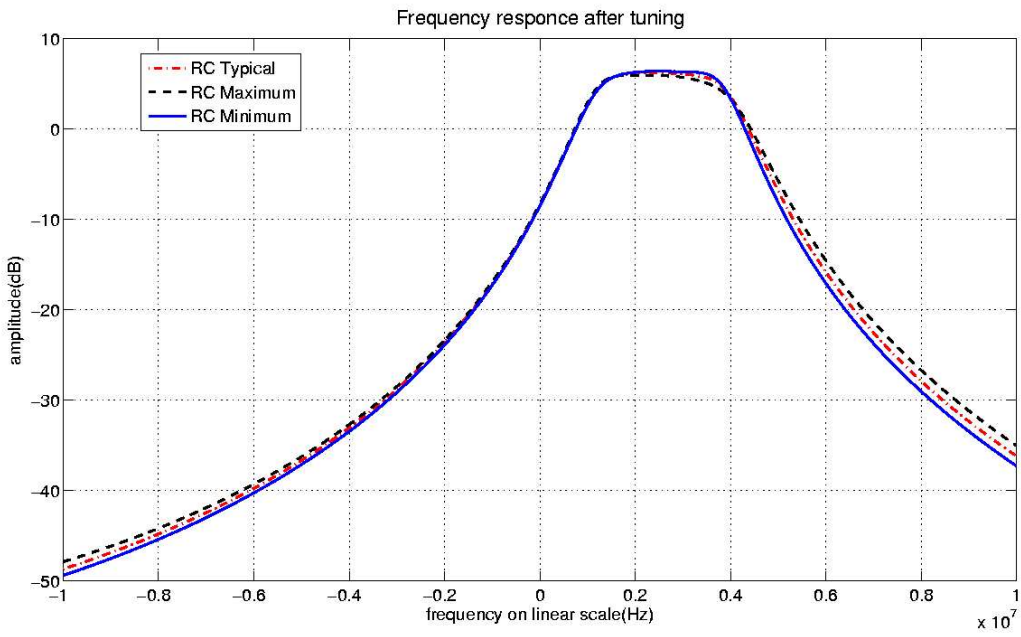

Figure 4.11: Frequency responce after tuning

CHAPTER 5

Results and Layout

In this chapter simulation results of the complex filter are explained and layouts of opamp and biquad filter were presented.

5.1 Mismatch analysis

The mismatch in real and imaginary paths results in imperfect cancellation of image frequency($-2.5MHz$) components at intermediate frequency($2.5MHz$). The maximum mismatch among resistances is 1% and the maximum mismatch among capacitors is 0.5%. The image responce at the output for 100 random iterations of montecarlo simulations for mismatch is shown in Fig. 5.1. Form these simulations the worst case image rejection is -46dB.

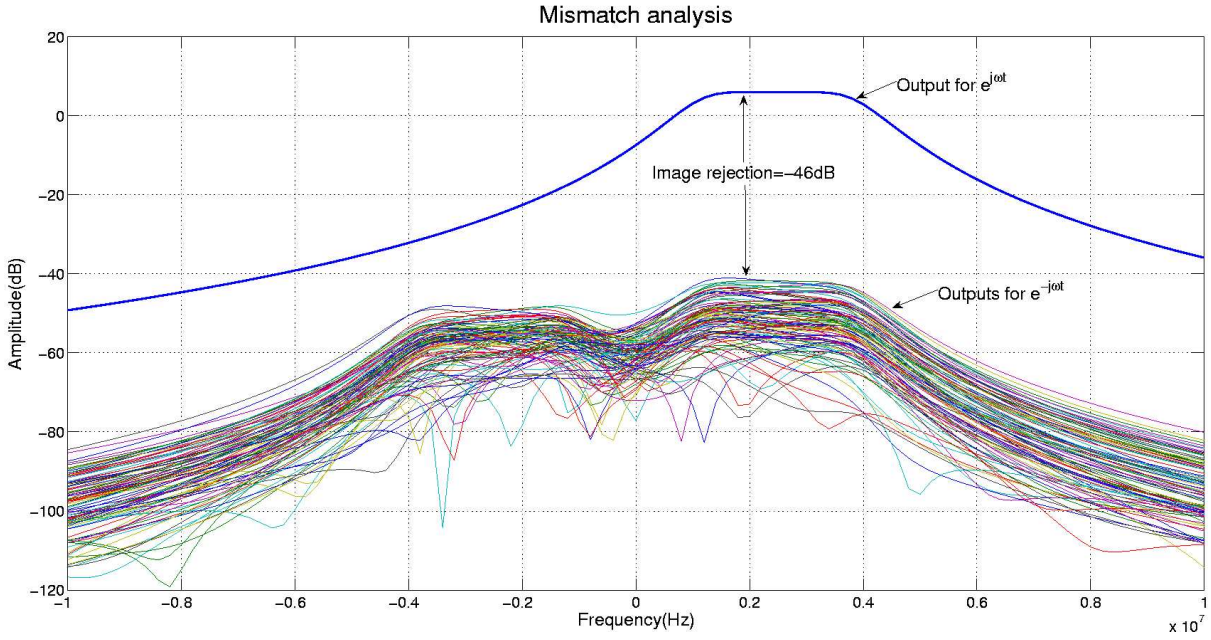

Figure 5.1: Image responce over 100 montecarlo simulations

From the response Fig. **??**, the output for the input $e^{j\omega t}$ is the frequency response of the complex filter. The outputs for the input $e^{-j\omega t}$ are the frequency response for negative frequency, leaking in to the positive frequency because of the imperfect cancellation of the image because of the mismatch between real and imaginary channels of the filter. For the 3^{rd} Butterworth complex filter the image rejection is $-46dB$.

5.2 Nonlinearity

The third harmonic distortion of the filter is estimated from the spectrum of the output of filter for single tone input at 2.5MHz with maximum input amplitude of 170mV single ended peak at minimum resistance corner. The spectrum is shown in Fig. 5.2. From the spectrum the output the third harmonic distortion is of -60dB, after tuning at minimum resistance and capacitance corner for output signal of $700mV$ peak to peak.

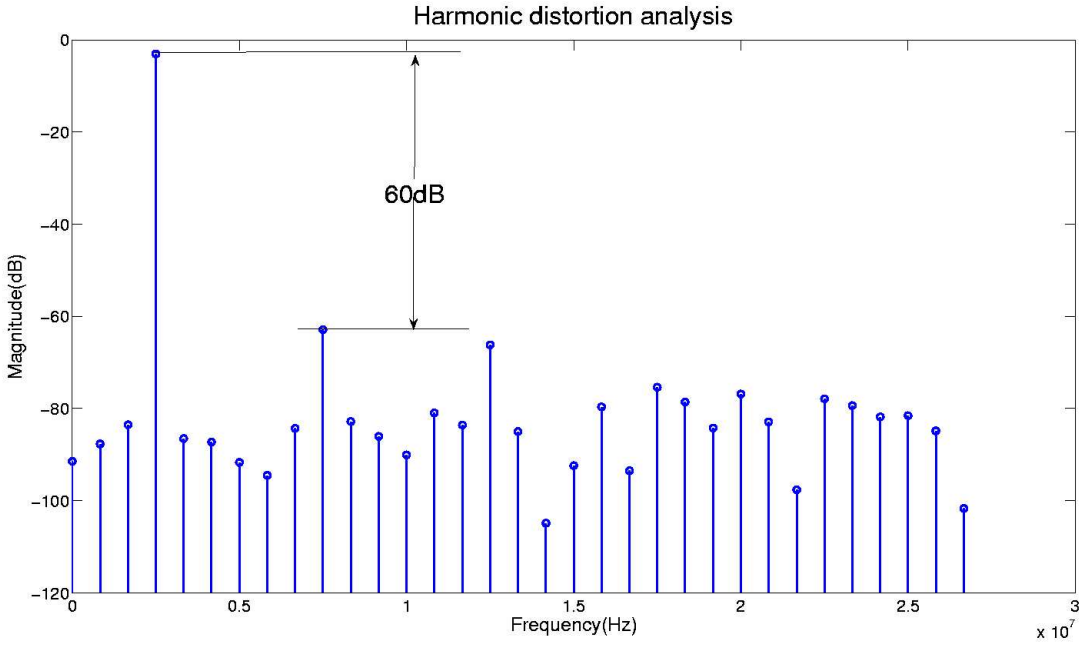

Figure 5.2: Filter output spectrum for single tone input

The intermodulation distortion of the filter is obtained by using two frequency

components $f_1 = 2.4MHz$ and $f_2 = 2.6MHz$ each with power of $-15dB$ as input to filter, and calculating spectrum of output of the filter and estimate the peaks at frequencies $2f_1 - f_2 = 2.2MHz$ and $2f_2 - f_1 = 2.8MHz$. The output spectrum of the filter output for two tones is shown in Fig. 5.3 for the input signal of $700mV$ peak to peak after tuning at minimum resistance and capacitance corner.

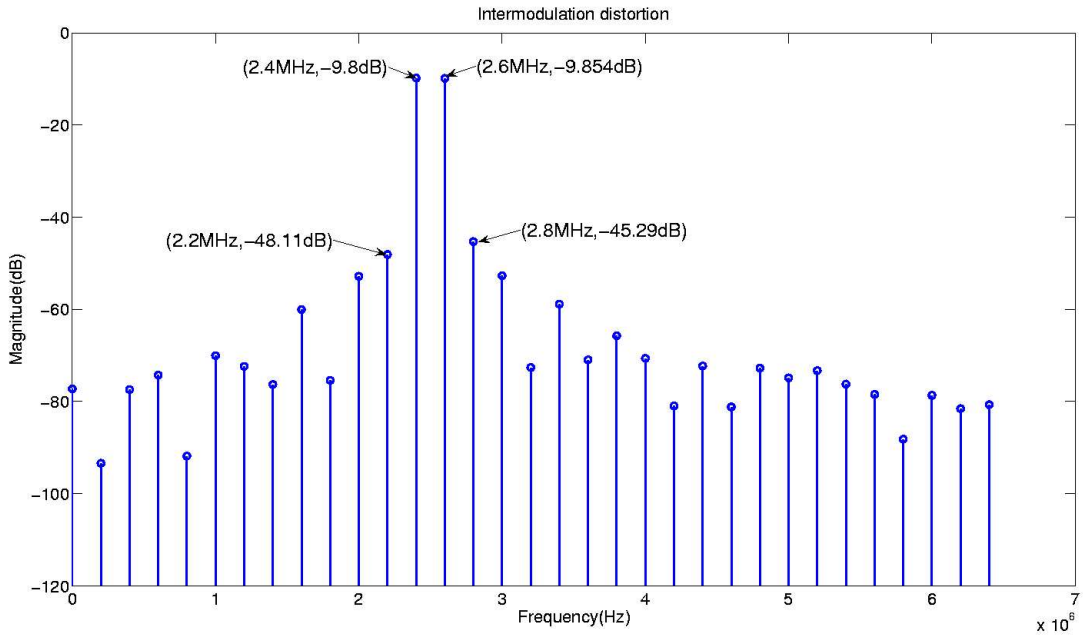

Figure 5.3: Intermodulation distortion spectrum

5.3 Comparison with zero-IF filter

The following Tab. 5.1 shows the main differences between zero-IF and low-IF filters.

5.4 Power consumption and noise

The main reason for the increase in the power consumption of the complex filter is requirement of SNR and dynamic range. The noise because of the complex biquad at the output of the filter was very high. To over come this problem the

Table 5.1: Comparison between zero-IF and low-IF filters

Parameter	Zero-IF	Low-IF
Filter Gain	0dB	6dB
DC Off-set suppression	0dB	-8.3dB
Power Consumption	1.34mW	3.51mW
Frequency of operation	0-1.5MHz	1MHz-4MHz
Input referred Noise (at temp=85°C and filter tuned for RC max corner)	$3.74X10^{-9}V^2$ (1KHz-1.5MHz)	$7.2X10^{-9}V^2$ (1MHz-4MHz)

first order complex filter which precedes the biquad was designed for gain equal to two. The first stage of the opamp used for complex biquad consumed of current of $80\mu A$ to meet the required noise specification. Since the noise because of the first order complex filter is very less, it did not require much noise optimization. But the opamp second stage was provided with $370\mu A$ of current each, to meet required linearity for $700mV$ peak to peak for load of $2.6K\Omega$ at lowest resistance corner. The power consumption of the opamp used for first order complex filter is $861\mu W$. Similarly the current in the second stage of the opamp used for the realization complex biquad filter was increased to meet the single ended swing of $700mV$. The power consumption of the opamp used for complex biquad filter is $822\mu W$. Hence the overall power consumption of the entire filter is $3.5mW$. The integrated input referred noise at one of the inputs of the complex filter is $V_{n_{RMS}} = 84\mu V$ integrated over the frequency of 1MHz to 4MHz, where as the minimum input voltage is $V_{in} = 790\mu V$ (5) (**?**) peak to peak.

5.5 Specifications of complex filter

Some of the important specifications were summarized in the Tab. 5.2.

Table 5.2: Specifications of the complex filter

Parameter	Specification
Frequency of operation	$1MHz - 4MHz$
Filter gain at $2.5MHz$	$6dB$
DC gain	$-8.3dB$
Adjscent channel suppressions	$-31.35dB$
Image rejection at 1% and 0.5% mismatch among resistances and capacitances	$-46dB$
THD(at 700mV peak to peak)	$60dB$
Intermodulation distortion(at 700mV peak to peak)	$35.4dB$
Power consumption	$3.2mW$
Integrated input referred Noise	$7.2 \times 10^{-9}V^2$ (1MHz-4MHz)

5.6 Layouts

The layout of the opamp for complex biquad is in Fig. 5.4. Its area on die is $106\mu mX63\mu m$.

The layout of opamp used for first order complex filter is in Fig. 5.5. Its area on die is $117.5\mu mX74.4\mu m$. The layout of complex biquad is in Fig. 5.6. Its area on die is $442\mu mX404\mu m$.

The layout of complex first order filter is in Fig. 5.7. Its area on die is $436\mu mX370.9\mu m$.

The layout of complete complex filter is in Fig. 5.8. Its area on die is $807.5\mu mX440.6\mu m$.

The resistances were modified from their theoretical values to restore the distorted frequency response after laying out the complex biquad to restore the distorted frequency response because of the parasitic capacitances, The resistance which is responsible for Q factor of the complex biquad adjustment is R_2. By hand tweeking it the required response. The modified values of the resistances of the complex biquad are as in Tab. 5.3.

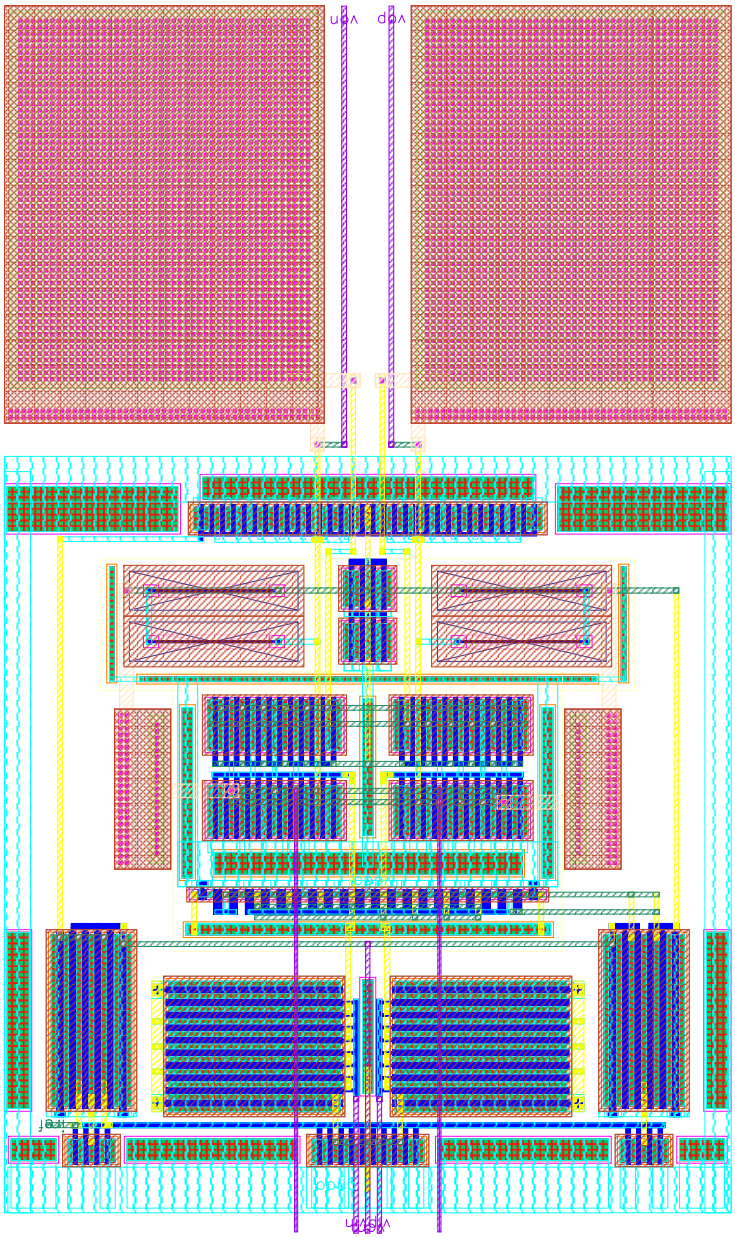

Figure 5.4: Layout of opamp used for complex biquad

Table 5.3: Biquad resistances optimized for after layout parasitics

Resistance	Value
R_1	$32K\Omega$
R_2	$7.18K\Omega$
R_3	$22K\Omega$
R_4	$22.8K\Omega$

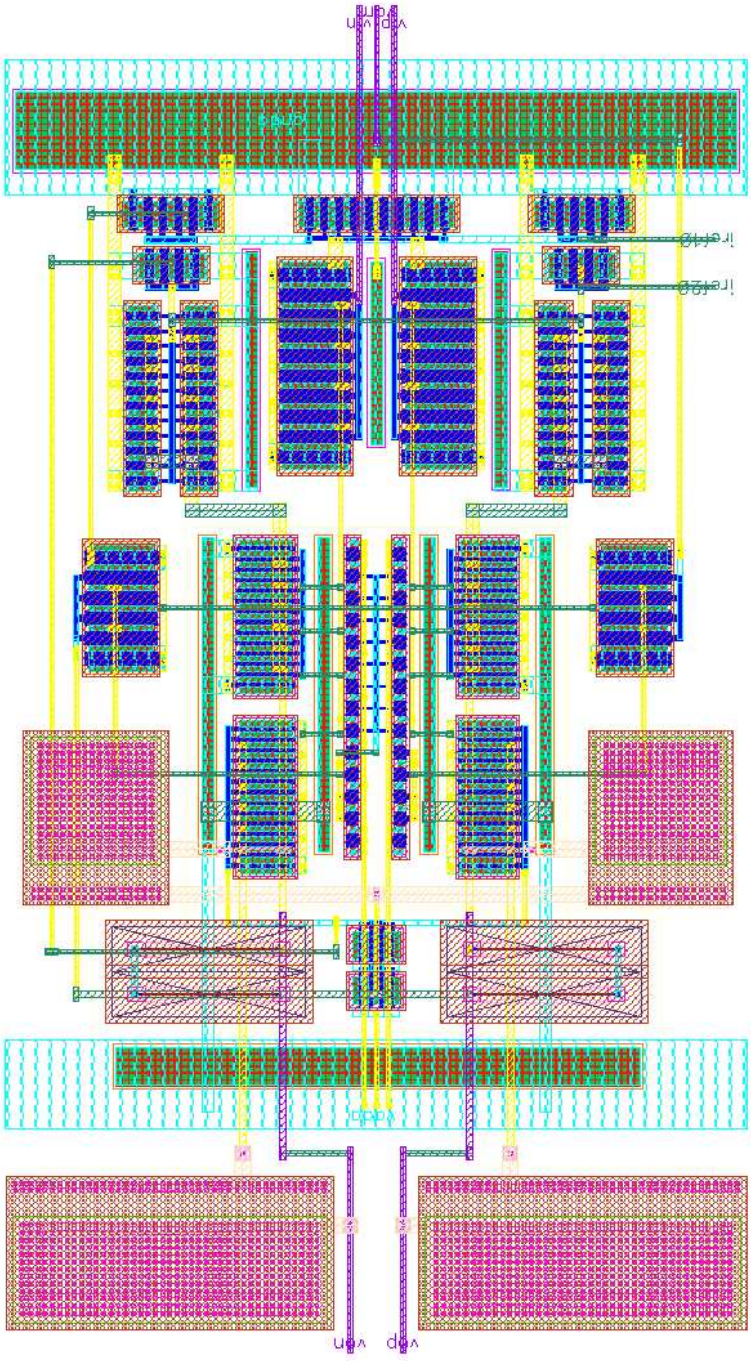

Figure 5.5: Layout of opamp used for complex first order filter

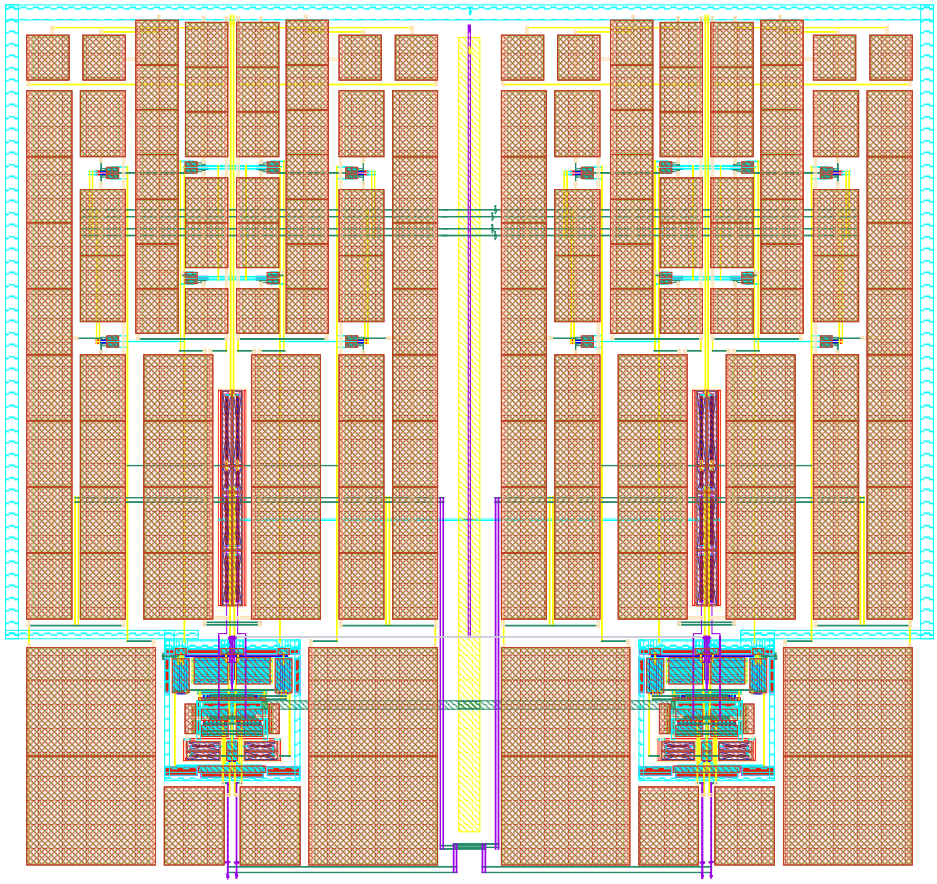

Figure 5.6: Layout of complex biquad

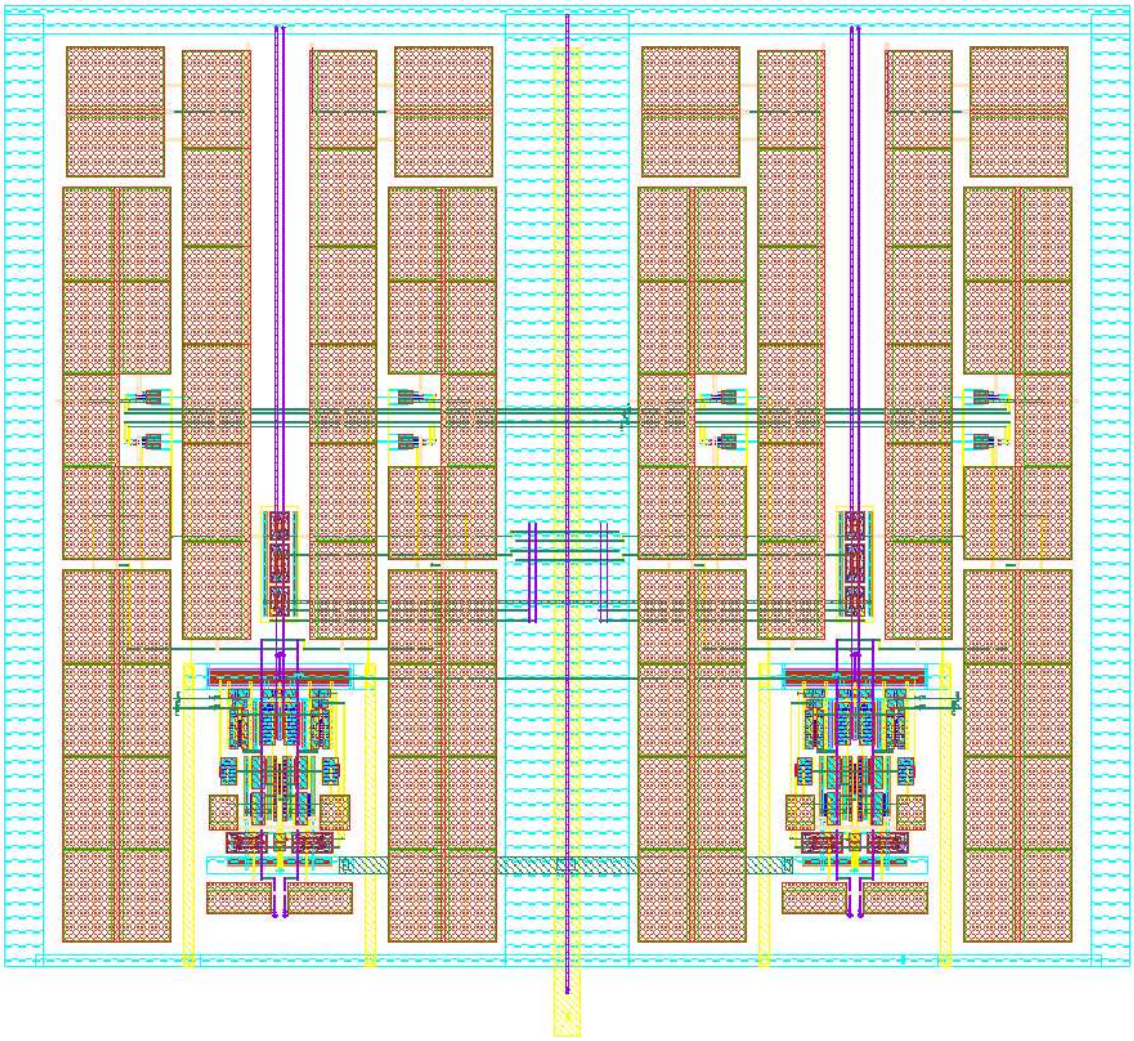

Figure 5.7: Layout of complex first order filter

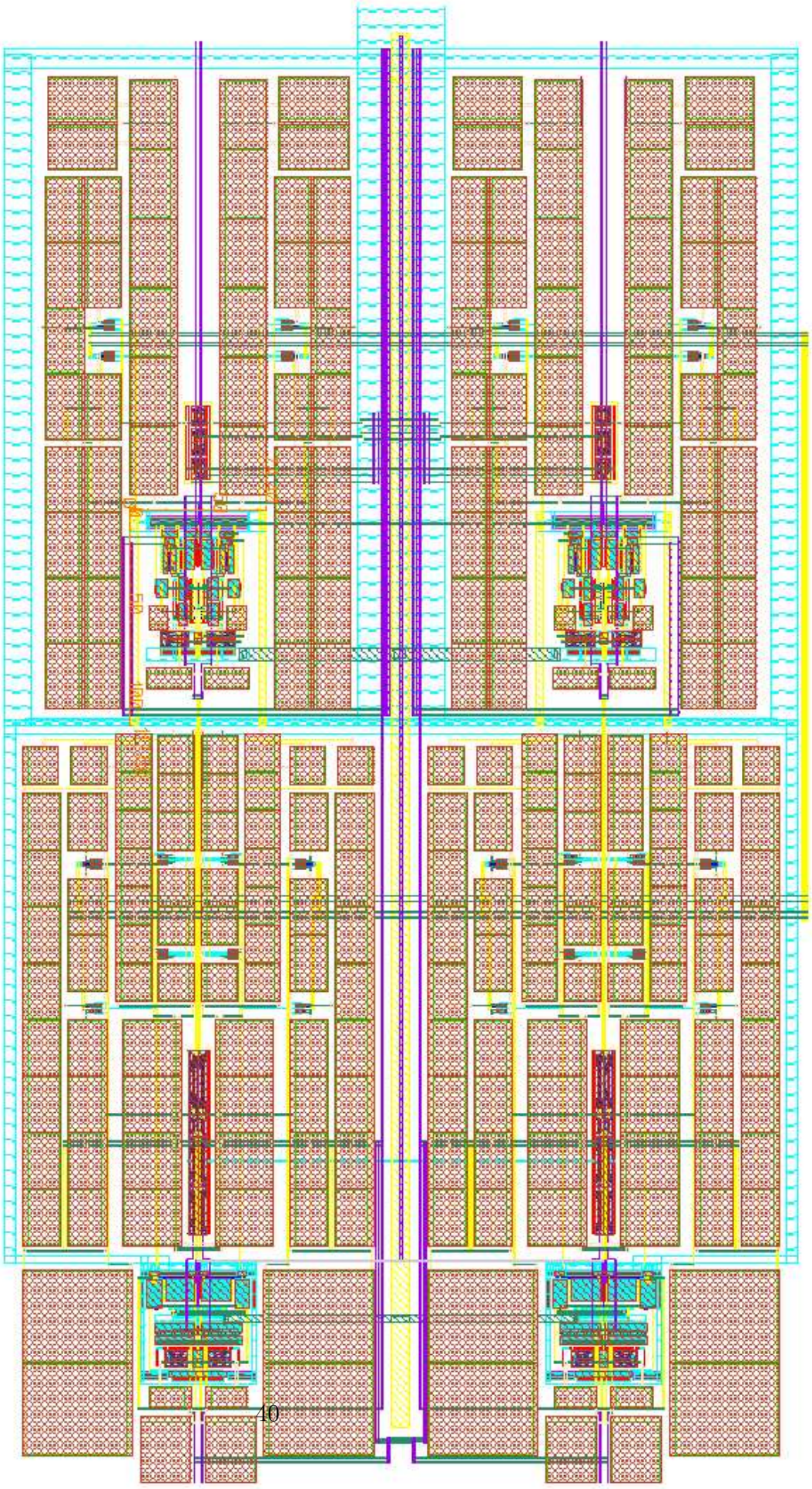

CHAPTER 6

Conclusion and Future Modifications

6.1 Conclusions

The power efficient complex filter for the low-IF IEEE 802.15.4 ZigBee transceiver was designed. The topology implemented was a first order compled filter followed by a complex biquad. To compensate for RC variations over process corners the capacitor tuning scheme controlled by four bits has been implemented. The noise and linearity specifications were satisfied. But compared to zero-IF architecture low-IF architecture because of higher power consumption.

6.2 Things to do

- ▷ Complete the layout of the filter.
- ▷ Interface the filter with mixer output and variable gain amplifier.
- ▷ Modify the clocking scheme of the ADC.

6.3 Future developments

- ▷ Static power can be minimized by implementing Class AB as second stage of opamp with a compromise over linearity.

REFERENCES

[1] K. Martin, "Complex signal processing is not complex," *IEEE Transactions on Circuits and Systems I: Fundamental Theory and Applications*, vol. 51, pp. 1823–1836, September 2004.

[2] M. J. G. Y. K. S. Linggajaya Kaufik, Do Manh Anh, "A new active polyphase filter for wideband image reject downconverter," *IEEE International Conference on Semiconductor Electronics*, pp. 213–217, December 2002.

[3] S. J. M. S. Jan Crols, "Low-if topologies for high-performance analog front ends of fully integrated receivers," *IEEE Transactions on Circuits and Systems-II: Analog and Digital Signal Processing*, vol. 45, pp. 269–282, March 1998.

[4] B. Razavi, *Design Of Analog CMOS Integrated Circuits*. Tata McGraw-Hill,New Delhi, 2002.

[5] S. Kumar, "Design of if stage for zigbee transceiver," p. 9, 2007.